ELSEVIER

Journal of Organometallic Chemistry 568 (1998) 21–31

Journal of Organometallic Chemistry

Torsional distortions in trimesitylsilanes and trimesitylgermanes

Joseph B. Lambert *, Charlotte L. Stern, Yan Zhao, Winston C. Tse, Catherine E. Shawl, Kirk T. Lentz, Lidia Kania

Department of Chemistry, Northwestern University, 2145 Sheridan Road, Evanston, IL 60208-3113, USA

Received 14 October 1997; received in revised form 27 May 1998

Abstract

The crystal structures have been solved for allyltrimesitylsilane (**3**), trimesitylsilane (**4**), and trimesitylgermane (**5**). Steric congestion caused by the three mesityl groups causes some lengthening of the Si–C and Ge–C bonds. The C–Si–C and C–Ge–C bond angles are increased when X is not H. Distortion is relieved by rotating the plane of the phenyl rings to create a propeller conformation. The same distortion has been found in unpublished data of the reported crystal structures of trimesitylsilyl azide (**6**) and aminotrimesitylgermane (**7**). Despite the variety of substituents (allyl, amino, azido, H) and the two different central atoms (Si, Ge), the twist angle of the propeller (compared with a conformation lacking any twist) lies between 41.6 and 48° for all five systems.

Keywords: Germane; Mesityl group; Propeller conformation; Silane; Steric congestion

1. Introduction

The propeller shape of (triaryl)M–X molecules (M = C, Si, Ge, Sn) is dictated by the interactions between substituents on the adjacent aryl rings, primarily *ortho–ortho* (**1**). If such interactions were absent, the six *ortho* carbons would all lie in a single plane just beneath the plane formed by the three *ipso* carbons (**2**).

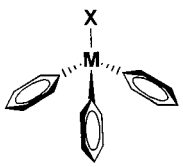

1

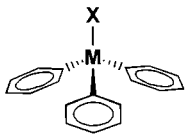

2

In order to minimize the *ortho–ortho* interactions, the plane of each arene ring rotates about the *ipso–para* axis so that the atoms or groups on the *ortho* carbons of a given ring alternate above and below (**1**) the plane of the six unrotated *ortho* carbons (**2**). These interactions increase when large substituents replace hydrogens in the *ortho* positions. Mesityl (2,4,6-trimethylphenyl; Mes), in which the *ortho* groups are methyl, has been widely used when steric bulk is required. When three such groups are present, as in trimesitylmethyl ($Mes_3C–$), the molecule is expected to exhibit considerable twisting about the *ipso–para* axes in the standard propeller geometry [1].

Trimesitylsilyl ($Mes_3Si–$) and trimesitylgermyl ($Mes_3Ge–$) have seen increased use as sterically bulky groups [2]. We have obtained the crystal structures of three such compounds: Mes_3Si-allyl (**3**), $Mes_3Si–H$ (**4**), and $Mes_3Ge–H$ (**5**). We report these structures herein and compare them with two similar structures already published in part: $Mes_3Si–N_3$ (**6**) [3] and $Mes_3Ge–NH_2$ (**7**) [4]. In particular, we report the respective twist angles of the arene rings for these five molecules.

2. Results

Trimesitylsilane (**4**) was prepared by the method of

* Corresponding author. Tel.: +1 847 4915437; fax: +1 847 4917713; e-mail: lambert@casbah.acns.nwu.edu

0022-328X/98/$19.00
PII S0022-328X(98)00754-2

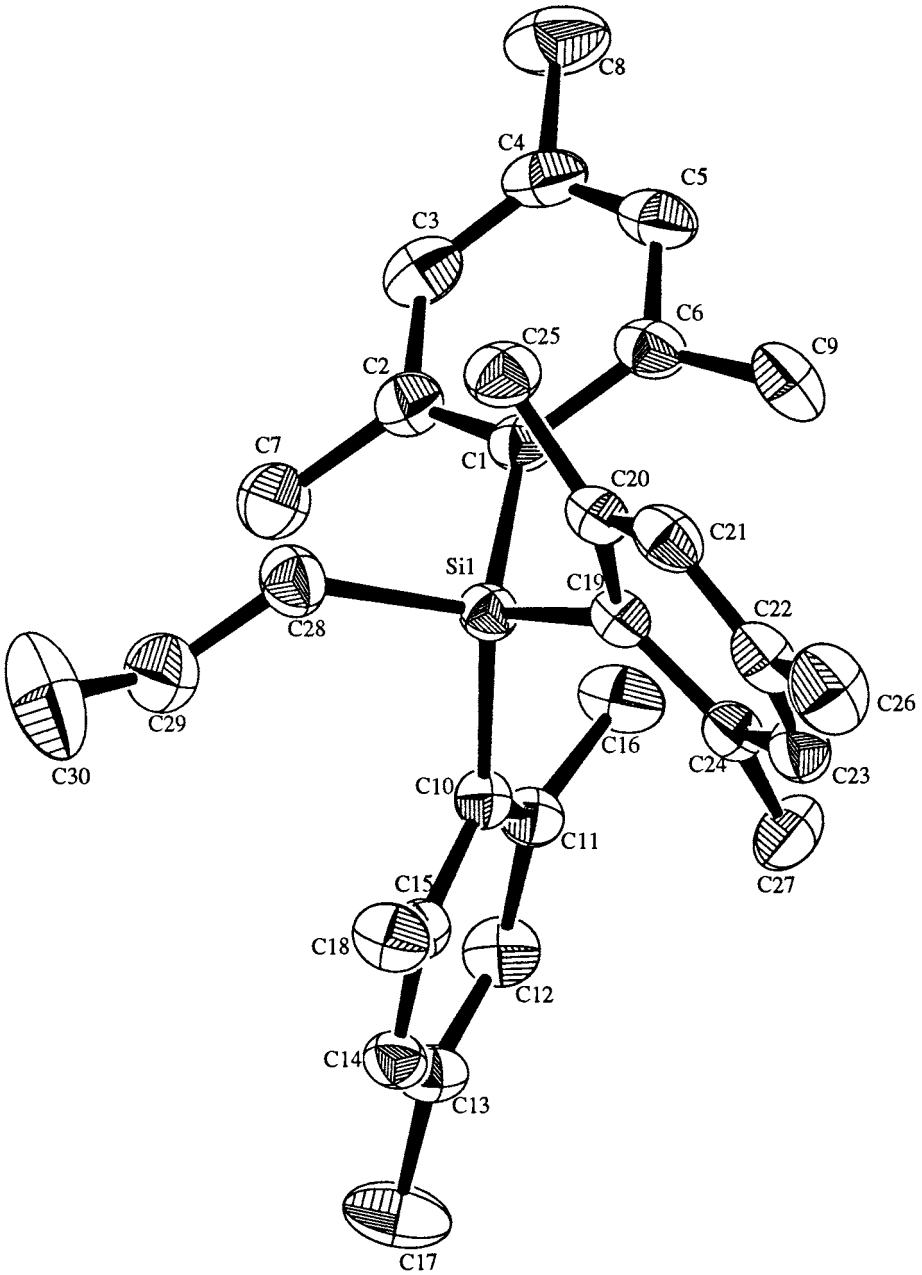

Fig. 1. Structure of allyltrimesitylsilane (**3**).

Lappert et al. [5] by the reaction of trichlorosilane with 2-bromomesitylene and sodium. Silane **4** was converted to chlorotrimesitylsilane with phosphorus pentachloride. Reaction of the chlorosilane with allyllithium yielded allyltrimesitylsilane (**3**) [6]. In a similar reaction sequence with germanium, trimesitylgermane (**5**) was obtained as a by-product. Suitable crystals for X-ray analysis were obtained for the allylsilane and the germane by slow evaporation of a solution of hexane and acetone. Common procedures for producing crystals only led to twins for trimesitylsilane. Vapor diffusion produced small crystals that gave weak reflections that did not permit anisotropic refinement (except with the silicon atom). Figs. 1–3 present ORTEP diagrams of **3**–**5**, respectively. Tables 1 and 2 present the atomic coordinates and significant structural parameters for the allylsilane **3**, Tables 3 and 4 for the silane **4**, and Tables 5 and 6 for the germane **5**. Tables 7 and 8 contain analogous data for the silyl azide [3] and the germylamine [4]. Most of these latter data did not appear in the original publications but were obtained from the Cambridge Crystallographic Database. Additional crystal data for **3**–**5** are found in Section 4.

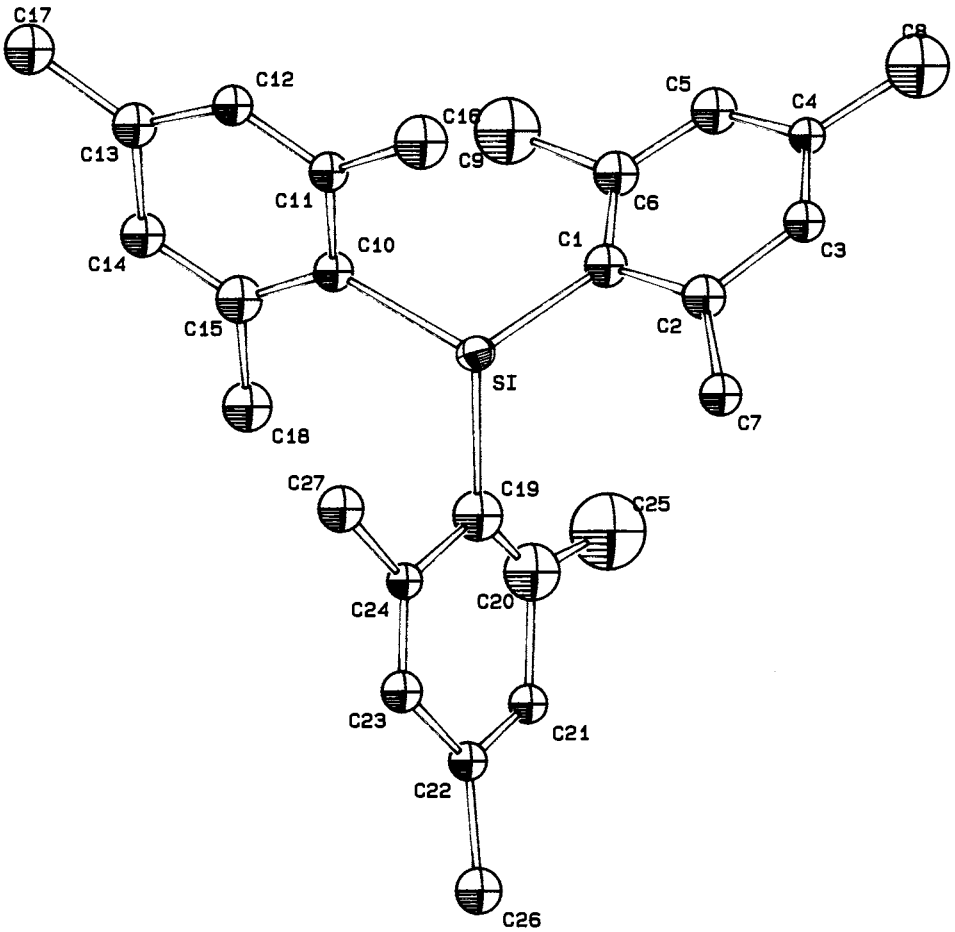

Fig. 2. Structure of trimesitylsilane (**4**).

3. Discussion

Table 9 assembles averages for the most relevant structural parameters: the M–C bond length, the C_i–M–C_i' bond angle, and the torsional angles through M (C_i–M–C_i'–C_o'). Distortions of each of these parameters could decrease steric interactions between adjacent aryl rings. For example, lengthening of the M–C bond would move the aryl rings further apart. The normal range for the C–Si bond is 1.86–1.91 Å [7], and the specific length in tetraphenylsilane is 1.872 Å [8]. The values for the allylsilane (1.909 Å) and the silyl azide (1.889 Å) are at the upper end of this range, as might be expected in sterically congested systems. The value for the silane **4** is about 0.1 Å above this range, but this result may be in part an artifact of the low level of isotropic refinement. The normal range for the C–Ge bond is 1.90–2.00 Å, and the specific value for tetraphenylgermane is 1.956 Å [9]. The value for the amine is at the upper end of this range, and that for the germane is above it. Thus, the M–C bonds for these mesityl systems tend to be longer than usual.

A second structural distortion to relieve steric interactions is enlargement of the C–M–C bond angle (the mesityl–M–mesityl angle) through flattening of the silicon or germanium tetrahedron, i.e., raising the C–M–C angle while lowering the C–M–X angle if the X group is smaller than mesityl (herein, X is allyl, H, amino, or azido). The C–Si–C angles for the allylsilane and the silyl azide are respectively, 112.9 and 114.0°, indicating a significant increase from tetrahedral. The value in the silane **4** is anomalously small, again possibly due to the poor refinement level. The germane **5**, however, is unperturbed at 109°. Thus the germane, and probably the silane **4**, with only a hydrogen for the fourth group X do not require angle distortion. The germylamine, like the two fully substituted silanes, has an enlarged angle, 113.9°.

The average angle (C–Si–X) from the allyl methylene carbon through the silicon atom to an *ipso* carbon in **3** (Fig. 1: C1Si1C28, C10Si1C28, and C19Si1C28 is 105.8°. In order for the mesityl groups to move further apart (C–Si–C is 112.9°), they must get closer to the fourth group (allyl), which is considerably smaller than the aryl groups. Thus the angles around silicon to the mesityl groups increase whereas those to allyl decrease. The analogous angles also are lower in the azide **6** (104.4°) [3] and in the amine **7** (104.7°) [4].

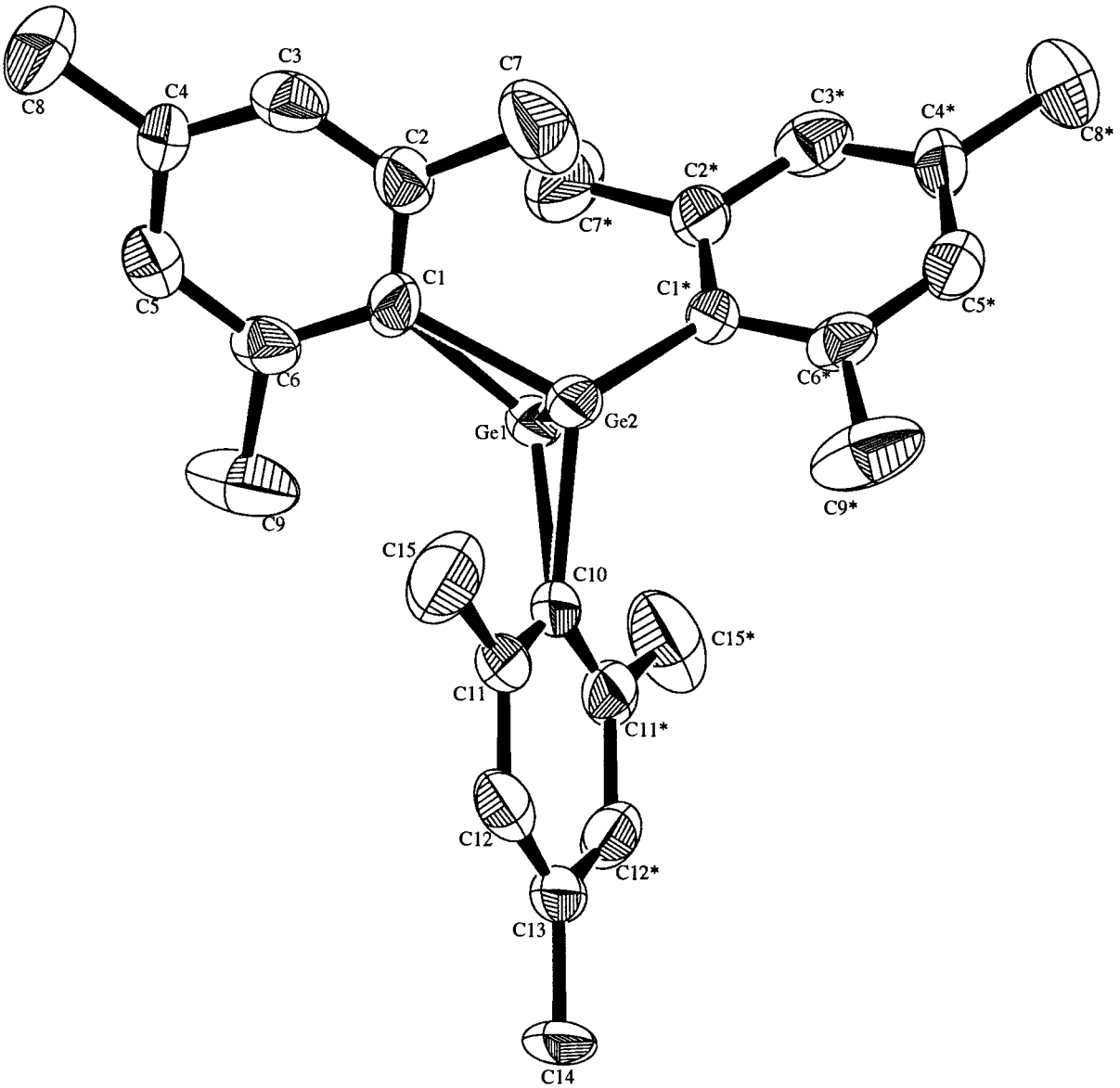

Fig. 3. Structure of trimesitylgermane (**5**).

Thus, the C–M–C angles involving the mesityl groups have expanded at the expense of the C–M–X angles involving the smaller fourth groups X.

The allyl group has other means to minimize steric strain. The C28–Si1 length is 1.919(3) Å, similar to the bond lengths from silicon to the mesityl *ipso* carbons but about 0.03 Å longer than the normal length. Hyperconjugation also may contribute to this bond lengthening. The allyl group extends itself by opening up bond angles. The Si1–C28–C29 angle is very appreciably increased to 124.7(2)° from 109.5° expected for an sp^3 carbon (although hyperconjugation again could contribute), and the C28–C29–C30 angle is slightly increased to 124.8(4)° from 120° expected for an sp^2 carbon. These distortions extend the allyl group, so that it is less bent and can allow closer approach of the mesityl groups. A similar distortion is seen in the azide **6**, in which the N–N–Si angle at 125.8° is increased by about 10° [3].

The various torsional or dihedral angles provide the most interesting insight into the steric effects. If each mesityl ring were symmetrically disposed as in **2**, the view along the *para–ipso* axis of one aryl ring into the plane of the other three atoms attached to M would resemble **8**. In this Newman projection, the *ortho* carbons with their attached methyl groups appear on either side with a dihedral angle between them of 180°.

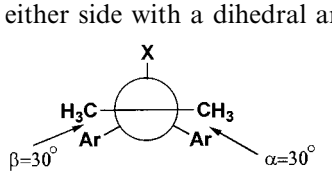

8

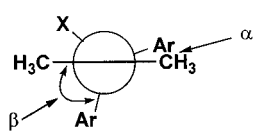

9

The dihedral angle between two rings, as defined by the angle between the C_{ipso}–M axis and the C'_{ipso}–C'_{ortho} axis of another ring (the C_i–M–C'_i–C'_o dihedral angle), is 30°, as illustrated by the angles α and β in **8**. This is the acute angle between the plane of the projected aryl ring and the M–C_{ipso} or M–C'_{ipso} axis in the illustrated Newman projection.

When the aryl ring twists to minimize the *ortho–ortho* methyl interactions, one of these angles (β) becomes larger than 30° and the other (α) becomes smaller than 30°. If this distortion is relatively large, as in all the present cases, one of the aryl rings passes to the other side of one C_o–CH_3 bond. The other aryl ring moves towards the perpendicular, as in **9**. The values of α and β are found three times in each molecule, representing the projection of each of the three mesityl rings onto the axes defined by the other two in **9**. The means of the three values are listed in Table 9.

The values of the more acute angle, α, range from 3.0 to 21.8°, and those of the less acute angle, β, range from 68.1 to 87° (to 81.8° if the silane **4** is excluded). The extent of the twisting distortion may be specified by comparison of the altered angles in **9** with the original angles in **8**. Thus, α moves from 30° past the C–Ar bond to an acute angle on the other side. The distortion thus is the sum $\alpha + 30$. The angle β also begins as 30° and increases to a large acute angle, so the distortion is the difference $\beta - 30$. The mean distortions may be calculated for each system and are given as ϕ in Table 9. Surprisingly, all six systems have very similar distortions, ranging only from 41.6 to 48° (to 45.0° if the silane **4** is excluded). Thus, the mesityl rings rotate some 41–45° to minimize *ortho–ortho* methyl interactions, irrespective of the metal M or the substituent.

The crystal structures are unremarkable except for the germane **5**. For both the silane **4** and the germane **5**, the hydride is not observed in the X-ray experiment. It is deduced to be present because no other atom appears at the fourth coordination site (no unaccounted for electron density), because the geometry around silicon or germanium is tetrahedral, and because no counterions are present. As Fig. 3 shows, there is disorder around the germanium atom. The disorder places the germanium atom both above and below the plane of the three *ipso* carbons to which it is attached. There is no disorder in the mesityl rings. Thus, exactly half the germanium tetrahedra point in one direction and half in the other, resulting in the observed presence of two half germanium atoms, represented in Fig. 3 by Ge1 and Ge2, with equal occupancy factors. If the germanium atom were a chiral center, there would be equal amounts of the two enantiomers.

Table 1
Atomic coordinates and B_{eq} for allyltrimesitylsilane (**3**)

Atom	*x*	*y*	*z*	B_{eq}
Si(1)	0.39038(9)	0.35217(3)	0.26338(5)	2.26(1)
C(1)	0.5238(3)	0.4102(1)	0.2189(2)	2.50(6)
C(2)	0.5636(3)	0.4032(1)	0.1243(2)	2.92(6)
C(3)	0.6481(4)	0.4473(1)	0.0846(2)	3.56(7)
C(4)	0.6983(3)	0.4976(1)	0.1349(2)	3.43(7)
C(5)	0.6649(3)	0.5034(1)	0.2287(2)	3.31(7)
C(6)	0.5817(3)	0.4610(1)	0.2722(2)	2.79(6)
C(7)	0.5256(5)	0.3489(2)	0.0632(3)	3.73(8)
C(8)	0.7926(6)	0.5433(2)	0.0908(4)	5.3(1)
C(9)	0.5649(5)	0.4727(2)	0.3775(3)	3.81(8)
C(10)	0.5013(3)	0.2794(1)	0.2874(2)	2.16(5)
C(11)	0.6751(3)	0.2713(1)	0.2931(2)	2.48(6)
C(12)	0.7403(4)	0.2156(1)	0.2947(2)	3.01(6)
C(13)	0.6451(4)	0.1666(1)	0.2950(2)	2.83(6)
C(14)	0.4778(3)	0.1748(1)	0.2976(2)	2.54(6)
C(15)	0.4057(3)	0.2291(1)	0.2953(2)	2.26(5)
C(16)	0.7991(4)	0.3206(1)	0.3020(3)	3.50(8)
C(17)	0.7185(5)	0.1071(2)	0.2944(4)	4.67(10)
C(18)	0.2265(4)	0.2314(2)	0.3096(3)	3.07(7)
C(19)	0.2978(3)	0.3768(1)	0.3725(2)	2.30(5)
C(20)	0.1632(3)	0.4169(1)	0.3552(2)	2.47(5)
C(21)	0.0676(3)	0.4257(1)	0.4267(2)	2.86(6)
C(22)	0.1010(3)	0.3973(1)	0.5168(2)	2.92(6)
C(23)	0.2434(4)	0.3629(1)	0.5383(2)	2.94(6)
C(24)	0.3428(3)	0.3528(1)	0.4696(2)	2.60(6)
C(25)	0.1194(4)	0.4537(1)	0.2623(2)	3.32(7)
C(26)	−0.0138(5)	0.4032(2)	0.5896(3)	4.29(9)
C(27)	0.5005(4)	0.3175(2)	0.5046(2)	3.57(8)
C(28)	0.1995(4)	0.3418(1)	0.1564(2)	3.22(7)
C(29)	0.1647(4)	0.2899(1)	0.0962(2)	4.07(8)
C(30)	0.0099(6)	0.2715(2)	0.0517(4)	7.0(1)

Table 2
Selected structural parameters for allyltrimesitylsilane (**3**)

Bond lengths (Å)	
Si1–C1	1.911(3)
Si1–C10	1.910(3)
Si1–C19	1.906(3)
Si1–C28	1.919(3)
C28–C29	1.454(4)
C29–C30	1.352(5)
Bond angles (°)	
C1Si1C10	113.2(1)
C1Si1C19	113.0(1)
C10Si1C19	112.4(1)
C1Si1C28	105.6(1)
C10Si1C28	107.5(1)
C19Si1C28	104.4(1)
Dihedral angles (°)	
C1Si1C10C11	12.9(3)
C1Si1C10C15	−163.6(2)
C1Si1C19C20	73.5(2)
C1Si1C19C24	−113.7(2)
C10Si1C1C2	66.7(2)
C10Si1C1C6	−115.6(2)
C10Si1C19C20	−156.9(2)
C10Si1C19C24	15.9(2)
C19Si1C1C2	−164.1(2)
C19Si1C1C6	13.7(3)
C19Si1C10C11	−116.6(2)
C19Si1C10C15	66.8(2)

Table 3
Atomic coordinates for trimesitylsilane (**4**)

Atom	*x*	*y*	*z*
Si	0.1024	0.0784(4)	0.9803
C1	−0.001(2)	0.162(2)	0.882(1)
C2	0.084(2)	0.132(2)	0.827(1)
C3	0.065(2)	0.203(2)	0.758(1)
C4	−0.006(2)	0.284(1)	0.748(1)
C5	−0.072(2)	0.308(2)	0.801(1)
C6	−0.065(2)	0.249(2)	0.867(1)
C7	0.179(2)	0.040(2)	0.827(1)
C8	−0.009(3)	0.350(3)	0.674(2)
C9	−0.132(3)	0.290(3)	0.931(2)
C10	0.052(2)	0.156(2)	1.068(1)
C11	0.140(2)	0.250(2)	1.081(1)
C12	0.152(2)	0.313(2)	1.145(1)
C13	0.096(2)	0.294(2)	1.204(1)
C14	0.011(2)	1.191(2)	1.189(1)
C15	0.004(2)	0.131(2)	1.124(1)
C16	0.227(2)	0.278(2)	1.030(1)
C17	0.110(2)	0.366(2)	1.275(1)
C18	−0.074(2)	0.030(2)	1.110(1)
C19	0.032(3)	−0.073(2)	0.971(2)
C20	−0.047(3)	−0.126(2)	0.926(2)
C21	−0.042(2)	−0.250(2)	0.929(1)
C22	0.037(2)	−0.304(1)	0.979(1)
C23	0.137(2)	−0.239(2)	1.034(1)
C24	0.137(2)	−0.135(1)	1.032(1)
C25	−0.162(4)	−0.087(4)	0.862(3)
C26	0.041(2)	−0.427(1)	0.972(1)
C27	0.237(2)	−0.068(2)	1.085(1)

Table 5
Atomic coordinates and B_{eq} for trimesitylgermane (**5**)

Atom	*x*	*y*	*z*	B_{eq}
Ge1	−0.0652(1)	0.0807(1)	0.24520(9)	2.68(3)
Ge2	0.0652(1)	0.0807(1)	0.25480(9)	2.68(3)
C1	0.0236(9)	0.1621(7)	0.3452(4)	4.3(2)
C1*	−0.0236(9)	0.1621(7)	0.1548(4)	4.3(2)
C2	0.1041(7)	0.2530(7)	0.3588(5)	3.8(2)
C2*	−0.1041(7)	0.2530(7)	0.1412(5)	3.8(2)
C3	0.1132(7)	0.3142(6)	0.4248(5)	3.9(2)
C3*	−0.1132(7)	0.3142(6)	0.0752(5)	3.9(2)
C4	0.0492(8)	0.2914(7)	0.4795(4)	3.8(2)
C4*	−0.0492(8)	0.2914(7)	0.0205(4)	3.8(2)
C5*	0.0257(7)	0.2002(7)	0.0322(4)	3.6(2)
C5	−0.0257(7)	0.2002(7)	0.4678(4)	3.6(2)
C6*	0.0382(7)	0.1356(6)	0.0980(5)	3.5(2)
C6	−0.0382(7)	0.1356(6)	0.4020(5)	3.5(2)
C7	0.1753(9)	0.2889(7)	0.3004(5)	7.0(3)
C7*	−0.1753(9)	0.2889(7)	0.1996(5)	7.0(3)
C8	0.061(1)	0.3591(8)	0.5512(5)	7.7(3)
C8*	−0.061(1)	0.3591(8)	−0.0512(5)	7.7(3)
C9	−0.1229(8)	0.0355(7)	0.3946(5)	6.6(3)
C9*	0.1229(8)	0.0355(7)	0.1054(5)	6.6(3)
C10	0.0000	−0.078(1)	0.2500	4.9(4)
C11	0.0946(8)	−0.1336(7)	0.3032(4)	3.7(2)
C11*	−0.0946(8)	−0.1336(7)	0.1968(4)	3.7(2)
C12	0.0913(7)	−0.2468(7)	0.3025(4)	3.7(2)
C12*	−0.0913(7)	−0.2468(7)	0.1975(4)	3.7(2)
C13	0.0000	−0.3060(9)	0.2500	3.2(3)
C14	0.0000	−0.4257(10)	0.2500	5.8(4)
C15	0.1996(9)	−0.0782(8)	0.3614(5)	6.9(3)
C15*	−0.1996(9)	−0.0782(8)	0.1386(5)	6.9(3)

This disorder may be explained either statically or dynamically. In the static explanation, the two structural modes must be present as a 50/50 mixture, for example, alternating along the stacks of molecular units. Alternatively, adjacent ribbons could have opposite senses. In the plane used for the depiction in Fig. 3, the molecules are arranged in columns (Fig. 4). In the

Table 4
Selected structural parameters for trimesitylsilane (**4**)

Bond lengths (Å)	
Si–C1	2.08(2)
Si–C10	2.00(2)
Si–C19	1.99(2)
Bond angles (°)	
C1SiC10	101.7(7)
C1SiC19	105(1)
C10SiC19	108.8(9)
Dihedral angles (°)	
C1SiC10C11	85(1)
C1SiC10C15	−124(2)
C1SiC19C20	2(4)
C1SiC19C24	−164(1)
C10SiC1C2	−157(1)
C10SiC1C6	12(3)
C10SiC19C20	−110(3)
C10SiC19C24	87(1)
C19SiC1C2	89(1)
C19SiC1C6	−125(3)
C19SiC10C11	−164(1)
C19SiC10C15	13(3)

Table 6
Selected structural parameters for trimesitylgermane (**5**)

Bond lengths (Å)	
Ge1–C1	2.049(7)
Ge1–C1*	2.031(9)
Ge1–C10	2.06(1)
Bond angles (°)	
C1Ge1C1*	106.6(3)
C1Ge1C10	109.8(2)
C1*Ge1C10	110.5(3)
Dihedral angles (°)	
C1Ge1C1*C2*	79.2(6)
C1Ge1C1*C6*	−118.4(8)
C1Ge1C10C11	5.3(7)
C1Ge1C10C11*	−158.7(5)
C1*Ge1C1C2	2.8(10)
C1*Ge1C1C6	−158.1(6)
C1*Ge1C10C11	−111.9(6)
C1*Ge1C10C11*	84.0(5)
C10Ge1C1C2	−116.8(8)
C10Ge1C1C6	82.2(6)
C10Ge1C1*C2*	−161.6(5)
C10Ge1C1*C6*	0.8(9)

Table 7
Selected structural parameters for azidotrimesitylsilane (**6**) [3]

Bond lengths (Å)	
Si–C1	1.887
Si–C10	1.892
Si–C19	1.888
Bond angles (°)	
C1Si1C10	113.3
C1Si1C19	115.1
C10Si1C19	113.7
Dihedral angles (°)	
C1Si1C10C11	68.0
C1Si1C10C15	−114.4
C1Si1C19C20	−165.7
C1Si1C19C24	16.1
C10Si1C1C2	−151.7
C10Si1C1C6	29.8
C10Si1C19C20	61.3
C10Si1C19C24	−117.0
C19Si1C1C2	75.1
C19Si1C1C6	−103.5
C19Si1C10C11	−158.1
C19Si1C10C15	19.4

first vertical column on the left, two mesityl groups point up and to either side (as in Fig. 3), while the third mesityl group points downward between the two mesityl groups of the next molecule. In the second column from the left, the order is reversed. One mesityl group points up and two point down and to either side. This arrangement optimizes the steric fit within the plane. The alternation continues, with the third column like the first, the fourth like the second, and so on.

Fig. 5 provides the view from a plane perpendicular

Table 8
Selected structural parameters for aminotrimesitylgermane (**7**) [4]

Bond lengths (Å)	
Ge–C1	1.973
Ge–C10	1.986
Ge–C19	1.976
Bond angles (°)	
C1GeC10	116.6
C1GeC19	113.0
C10GeC19	112.0
Dihedral angles (°)	
C1GeC10C11	−119.7
C1GeC10C15	66.7
ClGeC19C20	−157.7
C1GeC19C24	24.9
C10GeC1C2	19.8
C10GeC1C6	−158.5
C10GeC19C20	68.2
C10GeC19C24	−109.2
C19GeC1C2	−112.0
C19GeC1C6	70.7
C19GeC10C11	12.5
C19GeC10C15	−161.1

Table 9
Summary of structural parameters

	3	**4**	**6**[c]	**5**	**7**[d]
M	Si	Si	Si	Ge	Ge
X	$CH_2CH{=}CH_2$	H	N_3	H	NH_2
M–X (Å)	1.909	2.02	1.889	2.047	1.978
C–M–C (°)	112.9	105	114.0	109.0	113.9
α[a] (°)	14.2	9	21.8	3.0	19.1
β[a] (°)	69.0	87	68.1	81.8	68.5
ϕ[b] (°)	41.6	48	45.0	42.4	43.8

[a] See structure **9**.
[b] The average $0.5[(\alpha+30)+(\beta-30)]$.
[c] Data from the Cambridge Crystallographic Database from Ref. [3].
[d] Data from the Cambridge Crystallographic Database from Ref. [4].

to that of Fig. 4. Four rows of molecules are seen. Each row represents the molecules in the plane of Fig. 4, but now the molecules above and below that plane are visible in the rows above and below a given row. The disorder about germanium is seen from the diamond-shaped component at the center of each molecule. The view is along the *para–ipso* axis of one mesityl group. The other two mesityl groups extend to the left and right. Although it is not apparent in this perspective, the *para–ortho* axes alternate in front of and behind the plane of the perspective, as they represent molecules from adjacent columns of Fig. 4.

The dynamic explanation for the disorder is now seen from Fig. 5. In this plane the germanium atoms are positioned over each other from one row to the next. A hydride could move easily from one germanium atom to the next in the row above or below. This movement would precipitate hydride migration along the entire vertical column, inverting all the germanium tetrahedra. Both tetrahedral environments thus are populated, resulting in the observed disorder. By either the static or dynamic explanation, the crystal would exhibit equal amounts of the two forms on the average and lead to the structure of Fig. 3.

We emphasize that these explanations for the crystallographic disorder are unproved, and other explanations may be viable. One possibility is that the space group of trimesitylgermane (**5**) has lower symmetry than $C2/c$. Consequently, we also solved the crystal structure in the space groups Cc and $C2$. The disorder did not disappear in either solution. The germanium atom appears as two centers of electron density, with each site half occupied. For the $C2$ case, the residuals ($R = 0.083$, $R_w = 0.064$) are significantly larger than the values for the solution in $C2/c$ ($R = 0.068$, $R_w = 0.056$). In this space group the atoms on the $C2$ axis cannot be refined anisotropically. For the Cc case, the residuals ($R = 0.065$, $R_w = 0.048$) are comparable or better, but any improvement can be attributed to the additional parameters required by the model. For both alternative

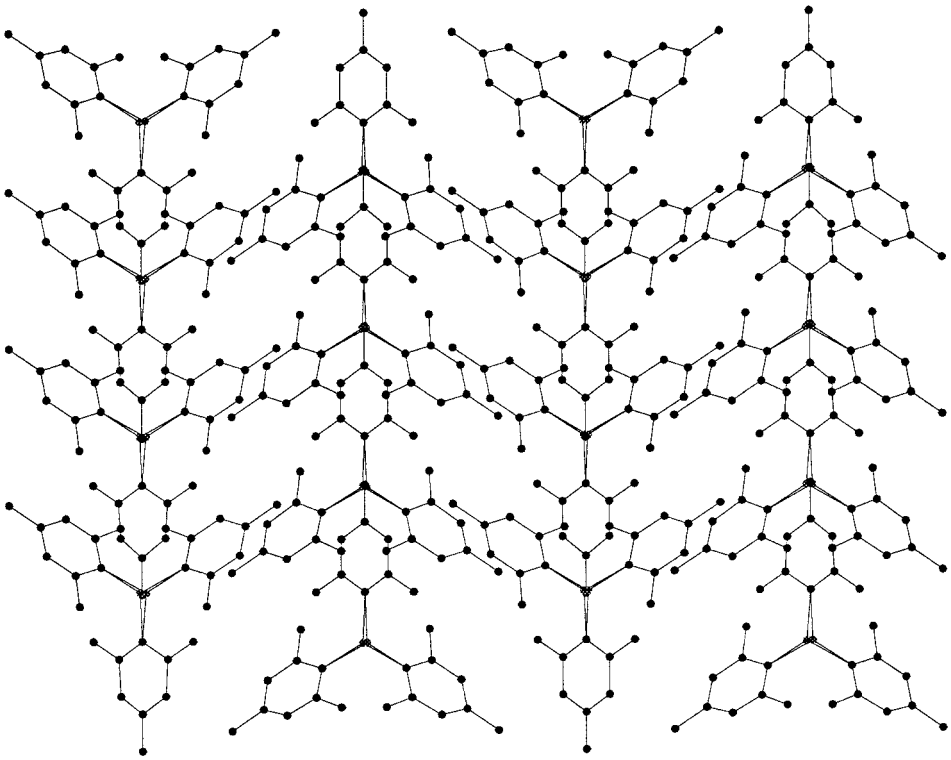

Fig. 4. View of one plane in the lattice of trimesitylgermane (**5**).

space groups, there are parameter correlations between all atoms. Furthermore, the $C2$ case has seven atoms and the Cc has ten atoms with nonpositive definite thermal coefficients that militate against acceptance. As a result, both space groups generate several unrealistic displacements ellipsoids.

The residuals, the parameter correlations, and the thermal coefficients all favor the $C2/c$ space group. Moreover, use of space groups with lower symmetry still results in disorder involving the germanium atom. This disorder thus appears to be real and requires a structural explanation such as the one we gave above. The problems of distinguishing between $C2/c$ and Cc have been discussed extensively by Marsh [10]. The poor quality of the data for trimesitylsilane (**4**) probably makes it impossible to render a distinction between the two. The preponderance of evidence for trimesitylgermane, however, strongly favors $C2/c$.

4. Experimental section

4.1. Trimesitylsilane (4) [5,11]

A 500 ml, three-necked, round-bottomed flask, equipped with a rubber septum, a condenser, and a glass stopper, was charged with powdered Na (4.8 g, 0.21 mol), 2-bromomesitylene (9.2 ml, 0.06 mol), dry benzene (150 ml) and a magnetic stirring bar. The flask was filled with N_2, and trichlorosilane (2.0 ml, 0.02 mol) was added through a syringe. The flask was heated slowly to 60°C, at which temperature an exothermic reaction occurred and the benzene began to reflux. The solution was then stirred overnight. The black suspension was filtered through a celite pad. The benzene solution was concentrated by rotary evaporation. The residue was crystallized from isopropyl alcohol to give 4.05 g (52.5%) of a white powder: mp 194°C, ^{1}H-NMR ($CDCl_3$) δ 2.12 (s, 18H), 2.26 (s, 9H), 5.73 (s, 1H), 6.78 (s, 6H); IR (KBr) Si–H 2140 cm^{-1}, MS (EI) m/z 386 (M^+, 2), 267 (25), 266 (91), 251 (46), 235 (32), 160 (33), 148 (16), 147 (97), 146 (100), 145 (32), 119 (24), 105(30). Anal. Calc. for $C_{27}H_{34}Si$: C, 83.93; H, 8.81; Si, 7.25. Found: C, 83.45; H, 8.99; Si, 7.10.

4.2. Chlorotrimesitylsilane [12]

A 100 ml, round-bottomed flask was charged with trimesitylsilane (1.35 g, 3.5 mmol), PCl_5 (1.12 g, 5.4 mmol), CCl_4 (30 ml), and a magnetic stirring bar. The mixture was heated to reflux under N_2 for 24 h. The solution was concentrated by rotary evaporation, and the residue was dissolved in hexane (50 ml). Methanol (15 ml) was added slowly to decompose the unreacted PCl_5. The organic layer was separated, dried over $MgSO_4$, and concentrated to give 1.22 g (83%) of a white solid: ^{1}H-NMR ($CDCl_3$) δ 1.96–2.46 (br, 18H), 2.24 (s, 9H), 6.72–6.90 (br, 6H).

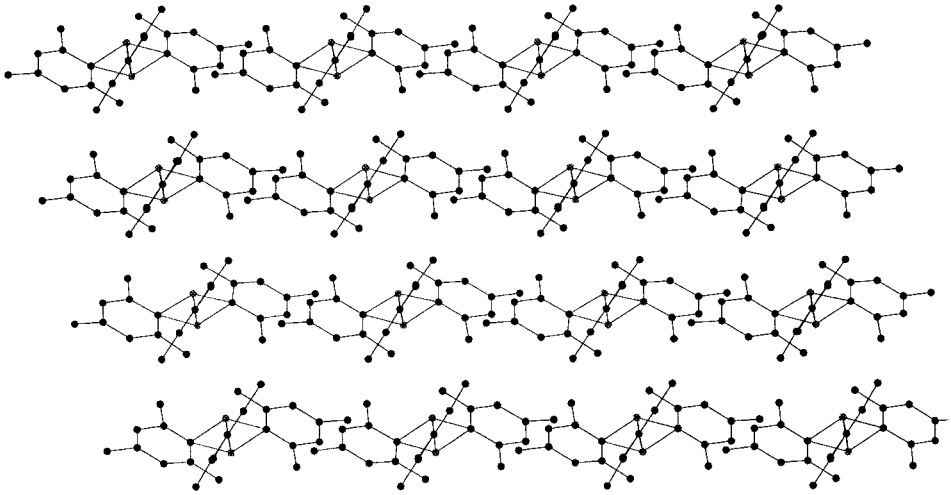

Fig. 5. View of a plane in the lattice of trimesitylgermane (**5**) that is perpendicular to the plane in Fig. 4.

4.3. Allyltrimesitylsilane (**3**)

A 100 ml, round-bottomed flask fitted with a rubber septum and a N_2 inlet needle was charged with allyltriphenyltin (8.55 g, 21.9 mmol) and a magnetic stirring bar. Anhydrous THF (50 ml) was added to the flask via a syringe. Phenyllithium (12.2 ml, 1.8 mol, 22.0 mmol) in ether and cyclohexane was then added quickly, and a large amount of precipitate (Ph_4Sn) formed immediately. After 0.5 h, the suspension was transferred through a wide-bore cannula to an enclosed glass frit under N_2 and was filtered into a 250 ml flask, which had been charged with chlorotrimesitylsilane (6.00 g, 14.4 mmol) and a stirring bar. The dark red solution was stirred at room temperature, and the reaction was monitored by ^{1}H-NMR. After 2 days, some chlorotrimesitylsilane was found to remain unreacted. Additional allyllithium (prepared as described above from 2.80 g of allyltriphenyltin and 4.0 ml of 1.8 M PhLi in 25 ml of THF) was added. After 1 day, all the chlorotrimesitylsilane was consumed. The reaction mixture was quenched by water and extracted with hexane (200 ml). The organic solution was dried ($MgSO_4$), concentrated, and chromatographed over silica gel with hexane as eluent to give a white solid (2.01 g, 33%): m.p. 160–163°C; ^{1}H-NMR (C_6D_6) δ 2.11 (s, 9H), 2.23 (s, 18H), 2.47–2.52 (m, 2H), 4.88–5.03 (m, 2H), 5.82–5.98 (m, 1H), 6.74 (s, 6H); ^{13}C-NMR (C_6D_6) δ 21.0, 25.5, 27.5, 116.2, 129.9, 135.7, 137.9, 138.6, 145.0; ^{29}Si-NMR ($CDCl_3$) δ −18.7l; Anal. Calc. for $C_{30}H_{38}Si$: C, 84.44; H, 8.98. Found: C, 84.30; H, 8.84.

4.4. Trimesitylgermane (**5**)

Trimesitylgermane was produced as a by-product of the preparation of allyltrimesitylgermane by the same method.

4.5. Crystal structure of trimesitylsilane (**4**)

Suitable crystals were extremely difficult to obtain. Numerous methods for purification and crystallization were tried, and efforts led only to crystals that were well formed but not single. Weakly reflecting crystals finally were obtained by placing 20 mg of **4**, dissolved in 2 ml of butanol, into a 2 d vial. This vial in turn was placed in a 10 d vial containing 5 ml of water. The larger vial was capped, so that water vapor could diffuse to the surface of the butanol. The single crystals of **4** appeared at the surface of the water-enriched butanol and were isolated. A white crystal of dimensions $0.35 \times 0.28 \times 0.08$ mm was used for the X-ray crystal determination. Measurements were performed on an Enraf-Nonius CAD4 diffractometer at −120°C with Mo–K_α radiation ($\lambda = 0.71069$ Å) by the ω–θ scan technique over a 2θ range of 4–55°. Cell parameters were determined by least-squares refinement of the setting angle of 25 high angle reflections. Further experimental details are given in Table 10. Intensities of three standard reflections measured every 3 h of X-ray exposure showed no significant decay. Intensity data were corrected for Lorentz polarization and absorption effects. Calculations were performed on a MicroVax 3600 with the teXsan 5.0 crystallographic software package [13]. The structure was solved by direct methods (MITHRIL) [14]. The full matrix least-squares refinement for all non-hydrogen atoms yielded an R factor of 0.148 ($R_w = 0.168$) for 1131 reflections with $I > 3\sigma(I)$ (2118 total reflections) and 116 variables. Because of the limited number of reflections, only the

silicon atom was refined anisotropically. The hydrogen atoms either were located from difference Fourier maps or were placed at the calculated positions. They were included in the final stage of refinement as fixed contributors to the structure factors. Final positional parameters and derived data are listed in Tables 3 and 4 with reference to Fig. 2.

4.6. Crystal structure of allyltrimesitylsilane (3)

A colorless crystal was obtained from the slow evaporation at room temperature of a solution of hexane and acetone. A colorless, tabular crystal with approximate dimensions of $0.48 \times 0.35 \times 0.20$ mm was mounted on a glass fiber using oil (Paratone-N, Exxon). All measurements were made on a Siemens SMART CCD diffractometer with graphite monochromated Mo–K_α radiation. Further experimental details are given in Table 10. Diffraction intensities were collected at -75 ± 1°C using the ω–θ scan technique to a maximum 2θ of 56.4°. Of the 16601 reflections that were collected, 6184 were unique ($R_{int} = 0.048$). The linear absorption coefficient for Mo–K_α was 1.1 cm^{-1}. Azimuthal scans of several reflections indicated no need for an absorption correction. The data were corrected for Lorentz and polarization effects. The structure was solved by direct methods and expanded with Fourier techniques [15,16]. Non-hydrogen atoms were refined anisotropically. Hydrogen atoms were refined isotropically. The final cycle of full-matrix least-squares refinement was based on 3965 observed reflections ($I > 3.00\sigma(I)$) and 432 variable parameters and converged with unweighted and weighted agreement factors of $R = 0.062$ and $R_w = 0.062$. The maximum and minimum peaks on the final difference Fourier map correspond to 0.28 and -0.26 e/Å^3, respectively. All calculations were performed using the teXsan crystallographic software package [13]. Structural parameters are given in Tables 1 and 2 with reference to Fig. 1.

Table 10
Crystallographic parameters

	3	4	5
M	Si	Si	Ge
X	Allyl	H	H
Formula	$C_{30}H_{38}Si$	$C_{27}H_{34}Si$	$C_{27}H_{34}Ge$
Molecular weight	426.72	386.65	431.16
Crystal system	Monoclinic	Monoclinic	C-centered monoclinic
Space group	$P2_1/c$ (No. 14)	Cc (No. 9)	$C2/c$ (No. 15)
a (Å)	8.1709(3)	11.107(3)	10.999(3)
b (Å)	23.1734(8)	12.171(1)	12.268(4)
c (Å)	13.7625(5)	17.525(3)	17.659(4)
β (°)	102.2541(9)	104.75(2)	104.69(2)
V (Å^3)	2546.5(1)	2291(1)	2304(1)
Z	4	4	4

4.7. Crystal structure of trimesitylgermane (5)

A colorless cubic crystal having approximate dimensions of $0.17 \times 0.24 \times 0.26$ mm was mounted using oil (Paratone-N, Exxon) on a glass fiber. All measurements were made on an Enraf-Nonius CAD4 diffractometer with graphite monochromated Mo–K_α radiation. Further experimental details are given in Table 10. The data were collected at a temperature of -120 ± 1°C using the ω–θ scan technique to a maximum 2θ value of 47.9°. Of the 2068 reflections that were collected, 1994 were unique ($R_{int} = 0.043$). The intensities of three representative reflections were measured after every 90 min of X-ray exposure time. No decay correction was applied. The linear absorption coefficient, μ, for Mo–K_α radiation is 13.4 cm^{-1}. An analytical absorption correction was applied, which resulted in transmission factors ranging from 0.72 to 0.80. The data were corrected for Lorentz and polarization effects. A correction for secondary extinction was applied (coefficient = 2.08373e − 07). The structure was solved by direct methods [15] and expanded using Fourier techniques [16]. Non-hydrogen atoms were refined anisotropically. Atom H16 (on germanium) was included from the difference map but not refined, and the remaining hydrogen atoms were included in idealized positions. The hydrogen attached to Ge and the remaining hydrogen on C14 were not included in structure factor calculations. The germanium was disordered off the twofold axis. The final cycle of full-matrix least-squares refinement was based on 1063 observed reflections ($I > 3.00\sigma(I)$) and 134 variable parameters and converged (largest parameter shift was 0.00 times its estimated S.D.) with unweighted and weighted agreement factors of $R = 0.068$ and $R_w = 0.056$. The maximum and minimum peaks on the final difference Fourier map corresponded to 0.38 and -0.34 e$^-$/Å^3, respectively. Structural parameters are given in Tables 5 and 6 with reference to Fig. 3.

Acknowledgements

This work was supported by the National Science Foundation (Grant No. CHE-9302747).

References

[1] For a review of propeller molecules, see K. Mislow, Acc. Chem. Res. 9 (1976) 26.

[2] For example, M.J. Fink, M.J. Michalczyk, K.J. Haller, R. West, J. Michl, Organometallics 3 (1984) 793.
[3] S.S. Zigler, K.J. Haller, R. West, M.S. Gordon, Organometallics 8 (1989) 1656.
[4] M. Rivière-Baudet, A. Morère, J.F. Britten, M. Onyszchuk, J. Organomet. Chem. 423 (1992) 5.
[5] M.J.S. Gynane, M.F. Lappert, P.I. Riley, P. Rivière, M. Rivière-Baudet, J. Organomet. Chem. 202 (1980) C5.
[6] J.B. Lambert, Y. Zhao, Angew. Chem. Int. Ed. Engl. 36 (1997) 400.
[7] W.S. Sheldrick, in: S. Patai, Z. Rappoport (Eds.), The Chemistry of Organic Silicon Compounds, Part 1, Wiley, Chichester, 1989, p. 245.
[8] C. Glidewell, G.M. Sheldrick, J. Chem. Soc. (A) (1971) 3127.
[9] (a) P.C. Chieh, J. Chem. Soc. (A) (1971) 3243. (b) P. Rivière, M. Riviere-Baudet, P. Satgé, in: G. Wilkinson (Ed.), Comprehensive Organometallic Chemistry, vol. 2, 1982, p. 502. (c) C. Glidewell, O.G. Liles, J. Organometal. Chem. 243 (1983) 291.
[10] (a) R.E. March, Acta Crystallogr. A 50 (1994) 450. (b) R.E. March, Acta Crystallogr. B 51 (1995) 897. (c) R.E. March, Acta Crystallogr. B 53 (1997) 317.
[11] J.J. Jerius, J.M. Hahn, A.F.M.M. Rahman, O. Mols, W.H. Ilsley, J.P. Oliver, Organometallics 5 (1986) 1812.
[12] S.S. Zigler, L.M. Johnson, R. West, J. Organomet. Chem. 341 (1988) 187.
[13] teXsan, Crystal Structure Analysis Package, Molecular Structure Corporation, 1985 and 1992.
[14] G.N. Gilmore, MITHRIL: A Computer Program for the Automatic Solution of Crystal Structures from X-ray Data, University of Glasgow, Glasgow, UK, 1983.
[15] G.M. Sheldrick, SHELX86, in: G.M. Sheldrick, C. Kruger, R. Goddard (Eds.), Crystallographic Computing 3, Oxford, 1985, pp. 175–189.
[16] P.T. Beurskens, G. Admiraal, G. Beurskens, W.P. Bosman, R. de Gelder, R. Israel, J.M.M. Smits, DIRDIF94: The DIRDIF-94 Program System, Technical Report of the Crystallography Laboratory, University of Nijmegen, The Netherlands, 1994.